Remote sensing techniques to assist the analysis of urban microclimate

Zina Mitraka[1], Foundation for Research and Technology – Hellas (Greece)
Jean-Philippe Gastellu-Etchegorry, Centre d'Etudes Spatiales de la Biosp – CESBIO (France)
Nektarios Chrysoulakis, Foundation for Research and Technology – Hellas (Greece)
Constantinos Cartalis, National and Kapodistrian University of Athens (Greece)

ABSTRACT

The increasing availability of Earth Observation (EO) systems and the advances in remote sensing technology have increased the opportunities for monitoring the urban environment and its thermal behaviour. Several parameters related to the urban climate can be derived from EO data, providing valuable support for advanced urban studies and climate modelling. Recently, attention has been drawn to the quantitative description of the urban thermal patterns and their correlations to fundamental surface descriptors. The potential of EO to support the analysis of urban microclimate by providing the means to identify Local Climate Zones (LCZ), remains underexploited. In this study, as a part of the project EO4SEB (Advanced Earth Observation techniques for urban Surface Energy Balance modelling), remote sensing techniques are applied to derive quantitative information needed to identify LCZ. Parameters like the pervious and impervious surface fraction, the surface albedo, the building density, the mean building/tree height and the sky view factor were quantified for a case study in a typical Mediterranean city, using satellite observations and ancillary information for the urban morphology. Having quantitative information on these parameters, enable the identification of possible zones in the urban fabric with relatively homogeneous thermal characteristics that can be considered as LCZ. Time series of land surface temperature estimates derived from satellite data are employed to identify thermal patterns and their correspondence to the LCZ.

Introduction

Data collected by Earth Observation (EO) satellites provides valuable source of information for understanding, monitoring, modelling and thus protecting the environment. The increasing availability of EO systems and the advances in remote sensing techniques have increased the opportunities for monitoring the urban environment and its thermal behaviour. The importance of EO in climate change studies has been recently discussed by Yang et al. (2013). Several parameters related to the urban climate can be derived from EO data, providing valuable support for advanced urban studies (Chrysoulakis 2003, Xu et al. 2008, Grau and Gastellu-Etchegorry 2013). Voogt and Oke (2003) on a review on application of thermal remote sensing in the urban areas, highlighted the need to advance research beyond qualitative description of thermal patterns and simple correlations and suggested to avoid qualitatively based land use data to describe the urban surface and focus on more fundamental surface descriptors. For example, an increase in Land Surface Temperature (LST) trend, despite the change in population, indicates that anthropogenic activities have been modified leading to higher anthropogenic heat flux in the city; it may be also attributed to land management changes, that is anthropogenic modification

[1] Corresponding Author: mitraka@iacm.forth.com, +30 2810 391762, Foundation for Research and Technology – Hellas (FORTH), N. Plastira 100, 70013 Heraklion, Greece.

without a change in land-cover type, as it has been recently described by Luyssaert et al. (2014). Grimmond et al. (2010) identified the needs for improvements in observations, data, understanding, modeling, tools and education to ensure that in the next 10 years we actively move towards developing more sustainable cities. Among others, Grimmond et al. (2010) identified the need to explore the use of new measurement techniques including the use of satellite remote sensing and the need to meet observation requirements to allow translation of research findings into urban community.

Recently, Stewart and Oke (2012) introduced a detailed classification scheme of Local Climate Zones (LCZ) based on various urban typologies, which explicitly defines urban landscapes according to their thermal properties. The scheme aims to be objective (incorporating measurable and testable features relevant to surface thermal climate), inclusive (sufficiently generic in its representation of local landscapes to not inherit regional or cultural biases) and standardized. The individual classes aim to have relatively homogenous air temperature within the canopy layer and they are defined by fact sheets with both qualitative and quantitative properties, including several features that can be derived from EO data. Bechtel and Daneke (2012) show that the LCZ can be determined from multiple EO data at local scale (100 m x 100 m).

An integration of the available remote sensing methods with numerical models and the combined use of EO and in-situ data may provide valuable insights to urban climatology. Coupling of different data sources and development of synergistic methods are necessary to overcome individual weaknesses and benefit from their diversity. To this end, an effort was recently made (Chrysoulakis et al. 2013); however, the potential of EO to support our understanding of the role of LCZ within the urban energy balance, to assist the analysis of urban microclimate, remains underexploited.

In this study, as a part of the project EO4SEB (Advanced Earth Observation techniques for urban Surface Energy Balance modelling), remote sensing techniques are employed to derive quantitative information, suitable for identifying LCZ in the city of Heraklion, Greece. The LCZ identification was based on a combination of EO-derived parameters such as the sky-view factor, the building density, the impervious and pervious surface fractions, the mean building/tree height and the surface albedo. Time series of LST estimates from satellite data were also used to identify the thermal footprint of the detected LCZ.

Study area and datasets

The study area is the city of Heraklion, the larger city in the island of Crete, Greece. It is a typical Mediterranean city with a rapidly growing urban agglomeration, consisted of a mixed land-use pattern that includes residential, commercial and industrial areas, transportation networks and rural areas. Fig. 1 shows the Urban Atlas land use map (Meirich, 2008) of the study area, overlaid to Google Earth. The surfaces corresponding to the developed areas are shown in blue, outlining the city core in the northern part of the study area. The surfaces corresponding to rural areas are shown in green. Apart from the Heraklion city core, the rest of the study area is featuring mixed urban and agricultural land cover pattern, mainly olive trees and vineyards. The study area (around 50 km^2) is outlined with the black polygon shown in Fig. 1.

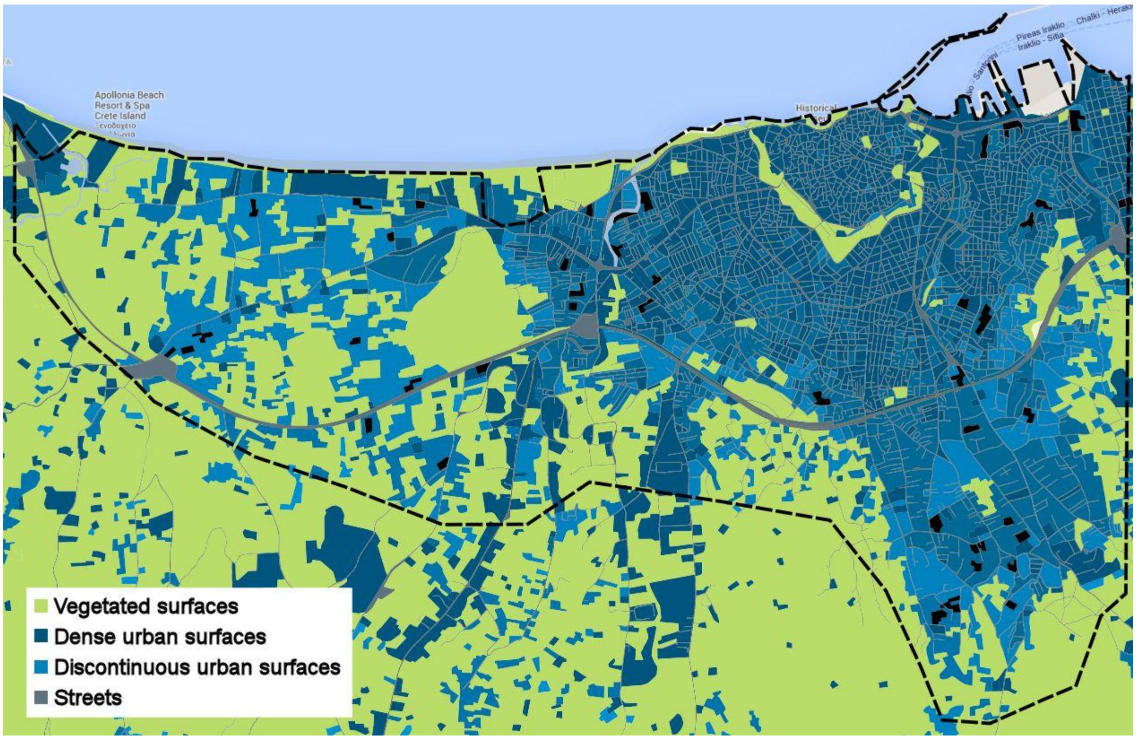

Figure 1. The study area outlined with a black dashed line, part of the city of Heraklion, Greece. Urban Atlas Land Use polygons are overlaid to Google Maps.

A Landsat-8 Level 1B image acquired over the study area (path: 181, row: 36) on 19 June 2013 (08:55 UTC) was used. Landsat-8 (Operational Land Imager – OLI) sensor consist of nine spectral bands, covering 0.43 – 1.38 μm, with a spatial resolution of 30 m. Detailed information on Landsat 8 sensor specifications and products is given by Roy et al. (2014). A Digital Surface Model (DSM) of 0.8 m and a Digital Terrain Model (DTM) of 5 m spatial resolution were available from the National Cadastre of Greece. Daily Moderate Resolution Imaging Spectroradiometer (MODIS) Level 1B data of 1 km spatial resolution, covering 10.78 – 12.27 nm, were also available for a period covering June 1, 2013 to December 31, 2013, from both Terra and Aqua satellites. The corresponding MODIS Level 2 Water Vapor products (MOD05) were also used to provide ancillary atmospheric information on water vapour and cloud cover. Surface cover abundance information from Landsat-8 Level 1B images covering the same time period were used to enhance the MODIS thermal measurements spatial resolution.

Methodology

In this section, the remote sensing methods used to derive the sky-view factor, the building density, the impervious and pervious surface fractions, the mean building/tree height, the surface albedo and the LST are briefly presented, followed by the approach used to identify the different LCZ.

Surface Parameters

Sky-view factor

The sky-view factor represents the fraction of sky hemisphere visible from ground level. It varies with height and spacing of buildings and trees and affects the radiational heating/cooling. The sky-view factor describes the ratio between the potential visible sky and the actual visible sky from a certain location, it depends on the height to width ratio of the street canyon and its values range between 0–1. There are some recent studies published that use EO data to estimate the sky-view factor. Rigo and Parlow (2007) for example used a digital elevation model to calculate it for use in heat flux modelling. Lindberg and Grimmond (2010) proposed a new method of calculation from high resolution urban DSM using a shadow casting algorithm. In this study, the sky-view factor was estimated in 0.8 m spatial resolution using the available DSM with a ray-tracing module of the ATCOR software (Richter and Schlapfer, 2012).

Building Density

Building density represents the proportion of ground surface with building cover. It affects the surface reflectivity, flow regimes and heat dispersion above ground. Various remote sensing methods exist that identify the buildings footprint from high resolution optical EO data or LiDAR data (Priestnall et al., 2000), from which building density can then be estimated. Recently, Kajimoto and Susaki (2013) used satellite radar data to directly quantify the building density of urban areas. In this study, the polygons of buildings footprint were available for the case study and building density was estimated in a grid of 30 m spatial resolution using GIS (Geographical Information Systems) analysis.

Impervious and Pervious Surface Fraction

Impervious and pervious surface fractions are the proportion of ground surface with impervious and pervious cover, respectively. Impervious and pervious surface fractions affect the albedo, the moisture availability and the heating/cooling rates. A large variety of remote sensing methods exist in literature to derive impervious and pervious surface fraction from EO data using different classification techniques (Weng, 2012). Methods based on spectral mixture analysis are proved valuable for estimating the surface cover type abundances from medium resolution satellite data (Ji and Jensen, 1999; Weng, 2009; Alonzo et al., 2014). The underlying urban landscapes are assumed to be composed of a few fundamental land cover components and their abundances are estimated by inverting the spectral mixture problem. In this study, Landsat multispectral data was used to estimate the impervious and vegetation surface fraction as per Mitraka et al. (2012). Four fundamental land cover components were assumed (i.e. vegetation, bright impervious, dark impervious and soil) and representative image collected spectra were used to invert the mixture problem. Impervious surface fraction was then estimated by combining the bright and dark impervious fractions at 30 m spatial resolution.

Mean Building/Tree Height

Mean building/tree height is the spatial average of building heights in an area of interest. It affects the surface albedo, flow regimes and heat dispersion above ground. The height of buildings and trees can be estimated from high spatial resolution DSM, given also information on the surface elevation. The finest and more accurate information on building/tree height can be derived using airborne LiDAR observations or high resolution stereoscopic imagery (Stal et al., 2013) from airborne sensors. DSM can also be constructed from satellite radar data, with a few limitations over urban areas (Wegner et al., 2014). In this study, information on building/tree height was estimated using the high resolution DSM, produced by stereo-analysis of airborne imagery, removing the terrain using the DTM, to retrieve the objects' height. Geometric mean was the estimated for a grid of 30 m spatial resolution covering the study area.

Surface Albedo

Surface albedo represents the surface ability to reflect the incoming direct and diffused irradiance at all wavelengths and towards all possible angles. Albedo is calculated as the bi-hemispherical reflectance of a surface and varies between 0 and 1 (unitless). Albedo affects the surface radiational heating potential, varies with surface colour, wetness and roughness (Schaepman-Strub et. al, 2006). If the Bidirectional Reflectance Distribution Function (BRDF) is known (or can be modelled) for a specific surface, its albedo can be estimated from EO data (Lucht et al., 2000), as the ration of the total reflected energy of the surface to the total incident energy on the surface (Van der Meer and de Jong, 2003). The atmospheric aerosol and water vapour content needed to estimate the fraction of the diffused radiation can be also retrieved from satellite observations (Jiménez-Muñoz et al., 2010). In this study, albedo was derived using the approach of Liang (2000) adjusted for Landsat-8 in 30 spatial resolution.

Land Surface Temperature (LST)

A spatial-spectral unmixing technique was applied to estimate time series of high spatial resolution LST (Mitraka et al., 2013) from MODIS thermal data. Such a technique is necessary to benefit from the high temporal resolution of MODIS (daily observations), while preserving high spatial resolution, essential for discriminating between the urban elements. Information on surface cover fractions derived from Landsat-8 OLI images was used to enhance the spatial resolution of MODIS thermal data. Emissivity information for the different surface cover types, derived from the ASTER spectral library, was used to estimate high spatial resolution emissivity (Mitraka et al., 2012). LST was derived using the reconstructed high resolution MODIS thermal bands, estimated emissivity and atmospheric information from the MODIS water vapour product (MOD05) in a split-window approach (Jiménez-Muñoz and Sobrino, 2008).

Identification of LCZ

The multiple sources of information used for estimating the different parameters resulted in products of different scales. Thus, there was a need to set a common scale of calculations to further proceed with the identification of possible LCZ. A spatial resolution of 30 m was considered adequate for the purpose of this study, in accordance with the LCZ requirements and facilitating also calculations with parameters derived from the Landsat-8 image (30 m spatial resolution). Consequently, all derived parameters were aggregated to a grid of 90 m × 90 m cell spatial resolution using an averaging filter. Each grid cell was then classified, based on its sky-view factor, building density, impervious/pervious surface fraction, mean building/tree height, albedo, according to the categorization scheme proposed by Stewart and Oke (2012). For an urban geographic area to be identified as a LCZ it should have a minimum diameter of 400 – 1000 m (Stewart and Oke, 2012). In practice, a 5 × 5 cells (450 m × 450 m) moving window was considered around each 90 m × 90 m grid cell and if more than 60% of the cells was found to belong in the same LCZ, the whole window was assigned to that zone. An application with a graphical user interface was created to facilitate the identification of LCZ, provided the calculated parameters. It should be noted that although anthropogenic heat flux information is needed in the LCZ identification scheme of Stewart and Oke (2012), such data was not used in this study, because further research is needed to derive this parameter from EO. The synergistic exploitation of the expected Sentinels 2 and 3 missions seems promising to this direction.

Results and discussion

The different parameters estimated from EO data are shown in Fig. 2 (the sky-view factor, the building density, the impervious and pervious surface fractions, the mean building/tree height and the surface albedo). Those parameters were then used as described above to identify possible LCZ in the study area. Two urban LCZ were identified using the available parameters, and the rest of the case study remained unclassified. The resulting urban LCZ for the case study of Heraklion are shown in Fig. 3. Blue colour in Fig. 3 represents the LCZ3, while green the LCZ6. It is worth noticing here that just the "urban" zones of the LCZ classification were considered in this study. Moreover, the classification was based on the available parameters only, excluding for example the surface admittance or the anthropogenic heat flux, which are also crucial for the zones discrimination.

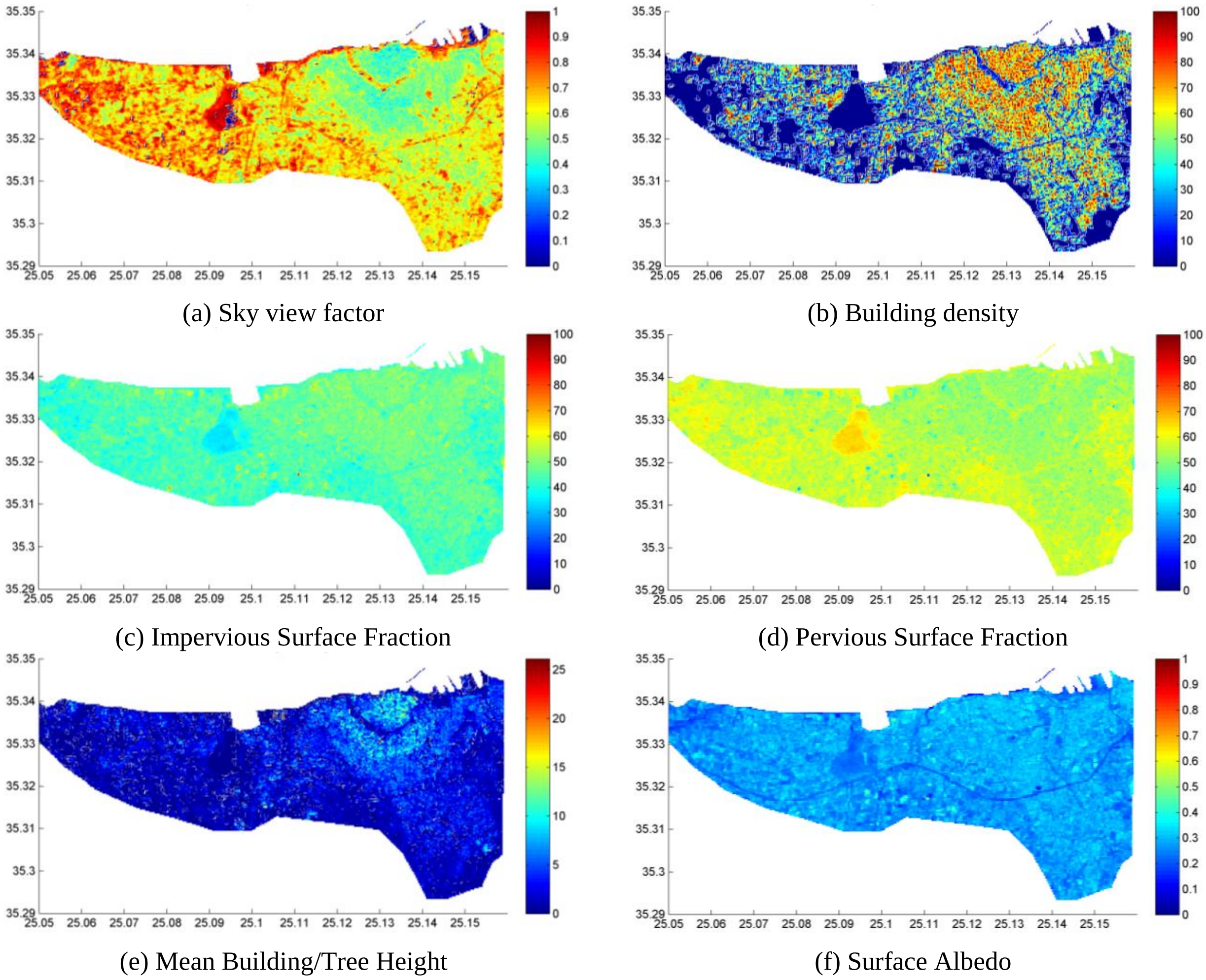

(a) Sky view factor

(b) Building density

(c) Impervious Surface Fraction

(d) Pervious Surface Fraction

(e) Mean Building/Tree Height

(f) Surface Albedo

Figure 2. Sky-view factor (a), building density (b), impervious (c) and pervious (d) surface fractions, mean building/tree height (e) and surface albedo (f), as estimated from the EO data.

The definition of LCZ3 describes it as an attached or closely spaced building area. The buildings of this zone are small (1-3 stories tall) and tightly packed along narrow streets. The sky view from street level is significantly reduced and heavy construction materials are used, like concrete, brick and tile. The land cover is mostly paved and hard-packed. There are few or no trees, moderate demand for heating and cooling and low to moderate traffic flow. The zone's function can be residential (single-unit housing, high-density terrace/row housing) and/or commercial (small retail shops) (Steward and Oke 2012).

LCZ3 seems to describe quite well the reality in the respective part identified in the study area (blue in Fig. 3). This area is both commercial and residential and its buildings are in most cases attached or otherwise closely spaced. Although in the city centre there are some taller buildings (5-6 stories tall), the majority is 2-3 stories tall with an average building height found in the area around 5 m. The mean sky-view factor from the street level found around 0.55 which is considered reduced, but not significantly, since it is found close to the upper bound in the definition of LCZ3 (0.6). The main construction materials are concrete, brick and tile, but information of the surface admittance would further corroborate this claim. There is also lack of vegetated surfaces in this area, apart from some street trees and small parks (see Fig. 1). Although there is a normal demand for heating, there is a high demand for cooling in the city, during the summer season and moderate traffic flow. Both heating/cooling demand and traffic flow effects were not captured in this study, because no anthropogenic heat flux data were used.

The definition of LCZ6 describes it as an area with small buildings of 1-3 stories tall, often in a grid pattern, the sky view from street level is slightly reduced and the construction materials vary (wood, brick, stone, tile). Scattered trees and abundant plant cover is observed. Low space heating/cooling demand and low traffic flow. Its function is mainly residential, with single or multi-unit housing, low density terrace/row housing or commercial with small retail shops (Steward and Oke 2012).

The definition of LCZ6 matches the description of the respective area identified in Heraklion (green in Fig. 3). The area is the periphery of the city of Heraklion and it is mainly a residential area. Buildings of maximum 3 stories tall are found here, with a mean sky-view factor of around 0.7. The construction materials used in this area are the same with the ones in the city core, but the lack of surface admittance data in the classification prevented further discrimination. Much more vegetation cover is observed in this zone compared to LCZ3, both scattered trees and abundant plants. Heating demand is normal due to mild winters, cooling demand quite high during summer and traffic flow is generally low in this area. Again, this kind of information could not be quantified in this study because of the lack of anthropogenic heat flux information.

Daily MODIS thermal measurements were disaggregated as described in the previous section and daily LST products were derived for the study area, for a period covering June 2013 to December 2013. Daily mean LST values were then extracted for each zone and their differences are shown in Fig. 4. Except from some extreme values in June and late October, LCZ3 and LCZ6 mean LST differences are less than 1 K. Higher mean LST values are observed in LCZ3 for June, July, September, October, November and December, while the situation is inversed for August 2013.

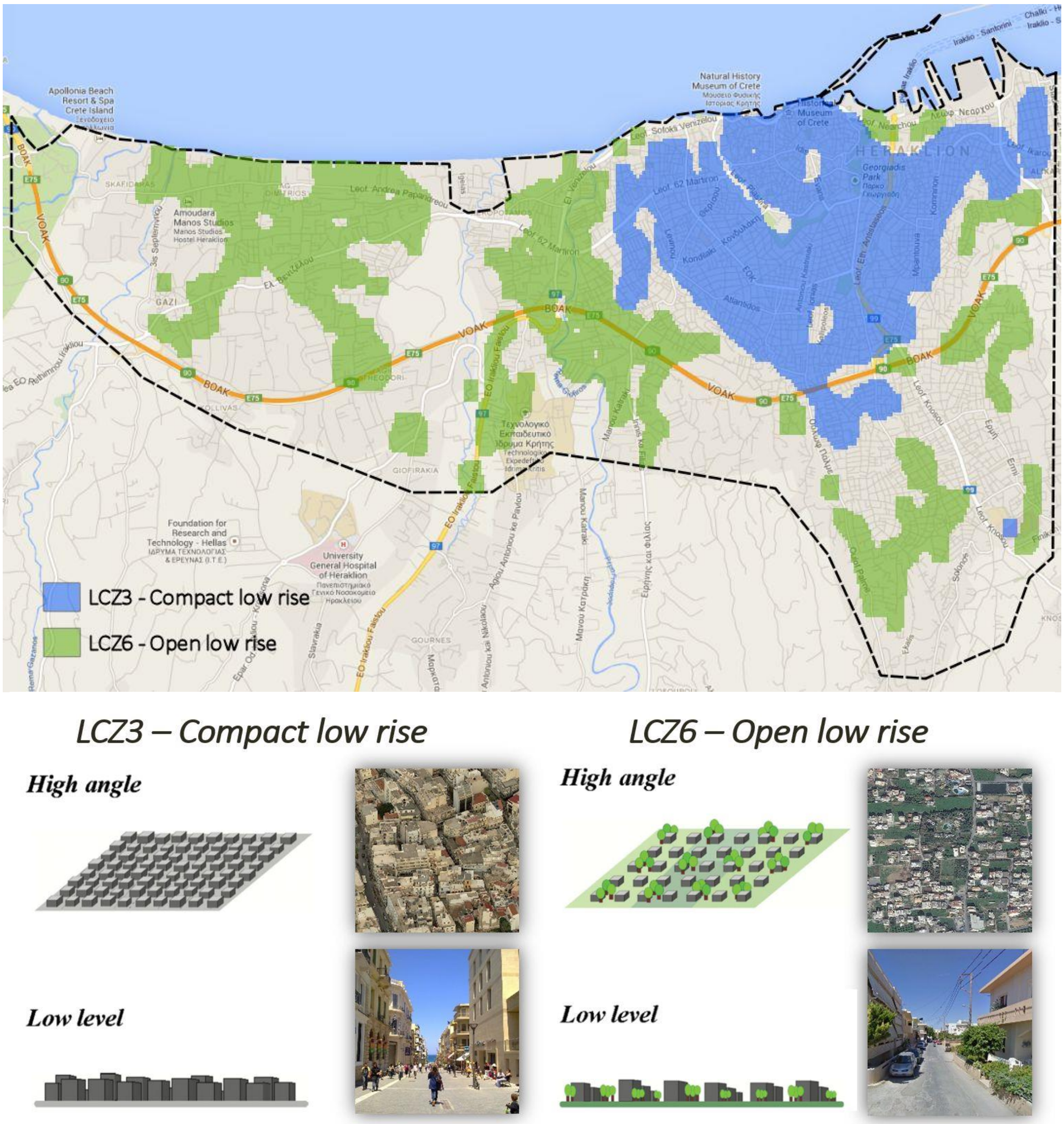

Figure 3. The spatial extend of the two urban LCZ identified in the case study, overlayed to Google Maps (top), blue corresponds to LCZ3 – Compact low rise, while green corresponds to LCZ6 – Open low rise and (bottom) their high angle and low level view (adapted by Steward and Oke (2012) and photos from Google Street-view and Bing Images)

The scope of this study is to outline a methodology for characterizing the LCZ by deriving each urban parameter using EO data and remote sensing science. More investigation is needed to come to conclusions about heat islands. Parameters like, the canyon aspect ratio, the terrain roughness, the surface admittance and the anthropogenic heat flux need to be quantified and taken into account to future studies. There is great potential of EO data for quantifying spatial patterns of those parameters. Moreover, both urban and rural LCZ should be considered for urban heat island studies, along with longer time series of night-time LST and air temperature measurements.

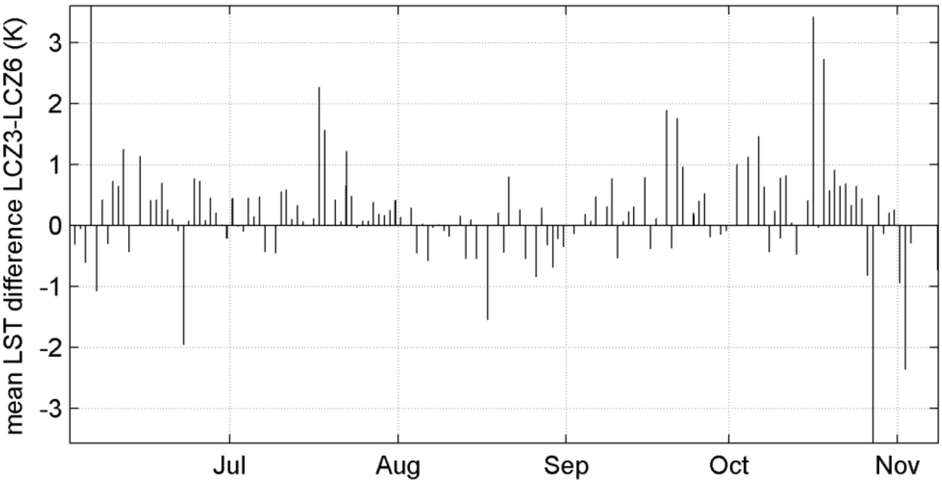

Figure 4. Differences of daily mean LST values (K) for LCZ3 – LCZ6.

Conclusions and further research

This is considered as a first attempt to demonstrate how the exploitation of EO data and remote sensing science can assist to quantify parameters related to the thermal behaviour of urban areas, with an ultimate goal to identify LCZ as defined by Steward and Oke (2012). More parameters like the surface roughness class, the surface admittance and the anthropogenic heat flux can be derived using EO data and standard meteorological measurements. Future research includes exploitation of EO data for estimating those parameters, as for example surface energy balance modelling for anthropogenic heat flux estimation. The ultimate goal is to develop a methodology to standardize input parameters for LCZ mapping. In this case EO will have the potential, through the LCZ estimation, to support well-established planning projects such as “climatope maps” (Scherer et al. 1999) and “urban climatic maps” (Ren et al. 2011).

Acknowledgment

This work was performed in the framework of the EO4SEB (Advanced Earth Observation techniques for urban Surface Energy Balance modelling) project within the O.P. Competitiveness and Entrepreneurship (Bilateral co-operation Greece- France) of the General Secretariat for Research and Technology of Greece (GRST code: 1309).

References

Alonzo, M., Bookhagen, B. and D.A. Roberts. 2014. “Urban tree species mapping using hyperspectral and lidar data fusion.” *Remote Sensing of Environment, 148*: 70–83.

Bechtel, B. and C. Daneke. 2012. "Classification of Local Climate Zones Based on Multiple Earth Observation Data." *IEEE Journal of Selected Topics in Applied Earth Observations and Remote Sensing,* 5: 1191 - 1202.

Chrysoulakis, N., Lopes, M., San José, R., Grimmond, C.S.B., Jones, M.B., Magliulo, V., Klostermann, J.E.M., Synnefa, A., Mitraka, Z., Castro, E., González, A., Vogt, R., Vesala, T., Spano, D., Pigeon, G., Freer-Smith, P., Staszewski, T., Hodges, N., Mills, G. and C. Cartalis. 2013. "Sustainable urban metabolism as a link between bio-physical sciences and urban planning: the BRIDGE project." *Landscape Urban Planning,* 112: 100 - 117.

Chrysoulakis, N. 2003. "Estimation of the all-wave Net Radiation Balance in Urban Environment with the combined use of Terra/ASTER multispectral imagery and in-situ spatial data." *Journal of Geophysical Research,* 108: D18, 4582.

Grau, E. and J. P. Gastellu-Etchegorry. 2013. "Radiative transfer modeling in the Earth–Atmosphere system with DART model." *Remote Sensing of Environment, 139,* 149 – 170.

Grimmond, C.S.B., Roth, M., Oke, T. R., Au, Y. C., Best, et al. 2010. "Climate and More Sustainable Cities: Climate Information for Improved Planning and Management of Cities (Producers/Capabilities Perspective)." *Procedia Environmental Science,* 1: 247 - 274.

Ji, M. and J.R. Jensen. 1999. "Effectiveness of Subpixel Analysis in Detecting and Quantifying Urban Imperviousness from Landsat Thematic Mapper Imagery." *Geocarto International, 14*(4): 33–41.

Jiménez-Muñoz, J-C. and J.A. Sobrino. 2008. "Split-Window Coefficients for Land Surface Temperature Retrieval From Low-Resolution Thermal Infrared Sensors." *IEEE Geoscience and Remote Sensing Letters, 5(4)*: 806–809.

Jiménez-Muñoz, J. C., Sobrino, J.A., Mattar, C., and B. Franch. 2010. "Atmospheric correction of optical imagery from MODIS and Reanalysis atmospheric products." *Remote Sensing of Environment*, *114*(10), 2195–2210.

Kajimoto, M., and J. Susaki 2013. "Global urban mapping using building density from polarimetric SAR images with POA correction". *Geoscience and Remote Sensing Symposium (IGARSS), 2013 IEEE International*: 4174–4177.

Liang, S. 2000. "Narrowband to broadband conversions of land surface albedo I: Algorithms." *Remote Sensing of Environment*, *76*, 213–238.

Lindberg, F., and C.S.B. Grimmond. 2010. "Continuous sky view factor maps from high resolution urban digital elevation models." *Climate Research*, *42*(3), 177–183.

Lucht, W., Schaaf, C. B., and A. Strahler, 2000. "An algorithm for the retrieval of albedo from space using semiempirical BRDF models." *IEEE Transactions on Geoscience and Remote Sensing*, *38*, 977–998.

Luyssaert, S. et al., 2014. “Land management and land-cover change have impacts of similar magnitude on surface temperature.” *Nature Climate Change*, *4*, 389–393.

Meirich, S. 2008. “Mapping Guide for a European Urban Atlas.” *GSE Land Information Services. GSE Land Consortium* http://www.ftsnet.it/documenti/740/mapping guide for a european urban atlas_EEA.pdf

Mitraka, Z., Berger, M., Ruescas, A., Sobrino, J.A., Jiménez-Muñoz, J.C., Brockmann, C. and N. Chrysoulakis. 2013. “Estimation of Land Surface Emissivity and Temperature based on Spatial-Spectral Unmixing analysis.” Proceedings of Sentinel-3 OLCI/SLSTR and MERIS/(A)ATSR workshop, Frascati, Italy (15-19 October)

Mitraka, Z., Chrysoulakis, N., Kamarianakis, Y., Partsinevelos, P. and A. Tsouchlaraki. 2012 “Improving the estimation of urban surface emissivity based on sub-pixel classification of high resolution satellite imagery.” *Remote Sensing of Environment*, *117*, 125–134.

Priestnall, G., Jaafar, J., and A. Duncan. 2000. “Extracting urban features from LiDAR digital surface models.” *Computers, Environment and Urban Systems*, *24*(2), 65–78.

Ren, C., Ng, E. Y. and L. Katzschner. 2011. “Urban climatic map studies: A review.” *International Journal of Climatology*, 31, 2213–2233.

Richter, R. and D. Schlapfer. 2012. “ATCOR-2/3 User Guide.” DLR - German Aerospace Centre, Remote Sensing Data Centre, Oberpfaffenhofen, Germany.

Rigo, G. and E. Parlow. 2007. “Modelling the ground heat flux of an urban area using remote sensing data.” *Theoretical and Applied Climatology*, 90:185–199.

Roy D. P. et al. 2014. “Landsat-8: Science and product vision for terrestrial global change research.” *Remote Sensing of Environment*, *145*, 154–172.

Schaepman-Strub, G., Schaepman, M. E., Painter, T. H., Dangel, S., and J. V. Martonchik, 2006. “Reflectance quantities in optical remote sensing-definitions and case studies.” *Remote Sensing of Environment*, *103*, 27–42.

Scherer, D., Fehrenbach, U., Beha, H.-D. and E. Parlow. 1999. “Improved concepts and methods in analysis and evaluation of the urban climate for optimizing urban climate processes.” *Atmospheric Environment*, 33, 4185–4193.

Stal, C., Tack, F., De Maeyer, P., De Wulf, A., and R. Goossens. 2013. “Airborne photogrammetry and lidar for DSM extraction and 3D change detection over an urban area – a comparative study.” *International Journal of Remote Sensing*, *34*(4), 1087–1110.

Stewart, I. D. and T. R. Oke. (2012). “Local Climate Zones for Urban Temperature Studies.” *Bulletin of the American Meteorological Society*, *93*(12): 1879–1900.

Voogt, J., and T. R. Oke. (2003). “Thermal remote sensing of urban climates.” *Remote Sensing of Environment*, *86*(3): 370–384.

Wegner, J., Ziehn, J., and U. Soergel. 2014. “Combining High-Resolution Optical and InSAR Features for Height Estimation of Buildings With Flat Roofs.” *IEEE Transactions on Geoscience and Remote Sensing*, *52*(9), 5840–5854.

Weng, Q. 2012. “Remote sensing of impervious surfaces in the urban areas: Requirements, methods, and trends.” *Remote Sensing of Environment*, *117*, 34–49.

Xu, W., Wooster, M.J. and C. S. B. Grimmond, 2008. “Modelling of urban sensible heat flux at multiple spatial scales: A demonstration using airborne hyperspectral imagery of Shanghai and a temperature–emissivity separation approach.” *Remote Sensing of Environment*, 112: 3493 - 3510.

Yang, J., Gong, P., Fu, R., Zhang, M., Chen, J., Liang, L., Xu, B., Shi, J., and R. Dickinson, 2013. “The role of satellite remote sensing in climate change studies.” *Nature Climate Change*, *3*, 875–883.